Kinetic Theory of Symmetry-Dependent Strength in Carbon Nanotubes

Georgii G. Samsonidze, Guram G. Samsonidze, and Boris I. Yakobson*

Department of Mechanical Engineering and Materials Science, Rice University, Houston, Texas 77005

(Received 29 July 2001; published 24 January 2002)

Carbon nanotubes yield to mechanical force by a primary dislocation dipole whose formation energy describes the thermodynamic stability of the tubule. However, the real-time strength is determined by the rate of defect formation, defined in turn by the activation barrier for the bond flip. First extensive computations of the kinetic barriers for a variety of strain-lattice orientations lead to predictions of the yield strength. Its value depends on nanotube chiral symmetry, in a way very different from the thermodynamic assessment.

DOI: 10.1103/PhysRevLett.88.065501 PACS numbers: 62.25.+g, 61.48.+c

Physics of strength and fracture remains a challenging area for many reasons [1]. It is an inherently multiscale phenomenon [2] that may begin from a few atoms involved in nucleation and ultimately evolves into macroscopic failure, often accompanied by complex patterns of cracks [3]. It can also begin and/or continue in an intermediate, mesoscopic scale of dislocations, preexisting in a macroscopic piece. The temporal aspects of this nonequilibrium process are crucial: How long a crystal can sustain a load before it gives is often more important than the formal thermodynamic stability. Here we address the kinetics of the very first event of yield, the formation of a primary defect that unlocks the perfect crystal for further relaxation. We chose a very small and simple while potentially important sample, an ultimate whisker, the carbon nanotube (CNT). Indeed, the strength and stiffness of CNT are among its appealing physical properties [4] especially in view of recent reports of a CNT-based actuator, resonator and microbalance, and a fiber [5]. Though tiny, CNT is likely to be the strongest material unit, and theory of its strength is essential.

Below we begin with the established atomic mechanism of relaxation in the graphene wall of CNT, nucleation of a dislocation dipole. The formation energy (E_f) of this defect is recalled, with an emphasis on symmetry dependence. In what follows, we underline the kinetic aspect of yield, and pose a question: How long does it actually take for the first defect to emerge, or how large a strain can CNT sustain before it yields and fails within laboratory time? To answer this, the activation barriers (E^*) and transition states (TS) must be considered in some detail. These values and geometries are computed, with the realistic multibody interatomic potential for a broad variety of applied stress magnitudes and orientations (to represent different chiralities of CNT). Based on these data, we show how kinetic treatment leads to the first quantitative evaluation of CNT strength limits. It is very different from thermodynamic predictions based on E_f, both in the magnitude of critical strain and in its strong dependence on chirality.

The way a monatomic sheet is rolled into a CNT can be specified by the diameter d and chiral angle χ between the cylinder circumference and the basis vector $\mathbf{a}_1$ in the lattice (Fig. 1a). All nonequivalent CNT chiral symmetries fall within the wedge $0 \le \chi \le \pi/6$. Notably, studies of elastic properties [6] have been greatly simplified by the fact that two-dimensional graphite crystals are elastically isotropic, so that moduli of CNT depend negligibly on chirality.

The situation changes qualitatively for large deformations causing irreversible atomic shifts. These nonlinear

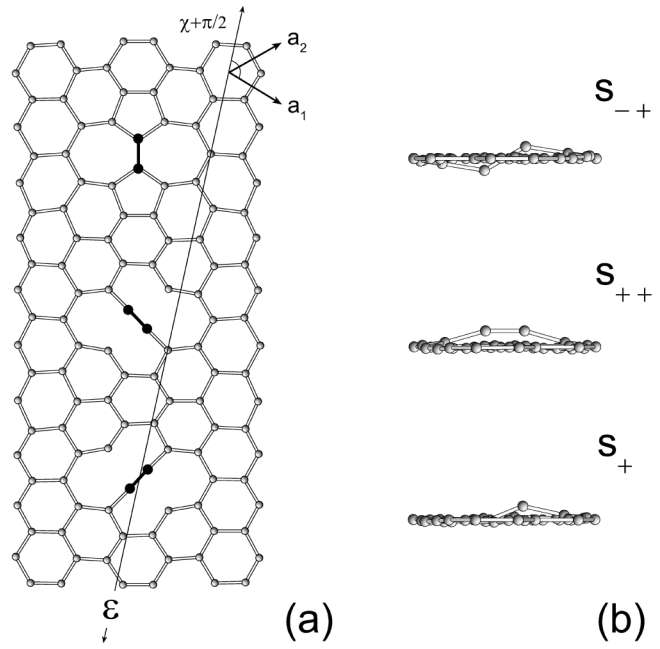

FIG. 1. (a) Atomic configurations for a 5-7-7-5 defect (top) resulting from the left (middle) or right (bottom) Stone-Wales rotation in graphene sheet. Corresponding transition states are aligned differently with respect to the tensile strain ε, directed at the angle $\chi + \pi/2$ from the basis vector $\mathbf{a}_1$ (in a nanotube of chirality χ; here $\chi = 19°$). (b) Modes S, S_{-+}, S_{++}, and S_+ all have a similar bond-rotation angle, but differ in the atom excursions out of plane (mode S not shown).

processes depend on strain direction with respect to the intrinsic hexagonal pattern and must vary with CNT chirality. Recent studies have identified the primary defect, responsible for CNT strength [7–9]. It is a 5/7 (pentagon/heptagon) dislocation dipole 5/7/7/5, produced by Stone-Wales (SW) $\pi/2$ rotation flip of a single C-C bond in a honeycomb lattice.

The SW defect has D_{2h} symmetry and is subject to the two fields in CNT: the external strain ε along the CNT, and the one due to cylindrical curvature, a/d, oriented at angles $\chi + \pi/2$ and χ with respect to $\mathbf{a}_1$, respectively. Based on symmetry analysis, the dependence of E_f on CNT chirality has been described [7,9,10]. Recent massive computations [11] have led to the approximation (omitting the d-dependent terms for brevity), $E_f(\varepsilon, \chi) = 2.72 - 3.9\varepsilon - 32\varepsilon \sin(2\chi + 30°) + O(1/d)$ eV. The significance of $E_f(\varepsilon, \chi)$ is its connection with the thermodynamic stability of strained CNT, which must therefore depend on chirality. One can define critical strain by the condition $E_f = 0$, when the SW defects (the nuclei of the failure) become favorable [8,10]. However, for this defect to emerge in real laboratory time (seconds or hours) the probability *rate* should be sufficient; that is the E^* must be reduced, a *kinetic* requirement more severe than the thermodynamic $E_f \leq 0$. Furthermore, the TS has lower symmetry than the final SW defect and therefore the chirality dependence of the strength is qualitatively different from the assessments based on E_f.

Computations of E^* must be guided by preliminary sampling of configurational space. SW flip has little effect on the surrounding lattice, so the transition should be sought between the ideal and SW-transformed geometries, near the $\pi/4$ rotation (Fig. 1a). Note that the left and right rotations lead to the same SW defect, but occur through different orientations with respect to the tension. In addition to in-plane rotation, the bond atoms can also move out of plane. Accordingly, a few basic modes must be considered. In the mode S, both flipping atoms stay in the plane. If they depart the plane in opposite directions (down, $-$, and up, $+$, Fig. 1b) this is mode S_{-+}. In the mode S_{++}, both atoms digress from the plane in the same direction. Finally, in the mode S_+, only one atom buckles out.

Structures of these modes and the corresponding E^* are computed in detail for the case of plane lattice only, in order to simplify the discussion. This is sufficient for the analysis of the role of chirality in CNT of finite diameters, while the precise E^* change little with curvature. (Similarly, analysis shows small E_f dependence on diameter [11,12].) We point out here that the degeneracy of the modes S_{++} (and S_{--}) and S_+ (and S_-) is lifted in a curved CNT, as the directions inward $(-)$ and outward $(+)$ become nonequivalent [13].

To model different chiralities, the strain is applied at the angles $\chi + \pi/2$. (The Poisson effect is also taken into account; note that for our supercell size 6 nm relaxation at constant stress yields energies within 0.02 eV from the constant strain results.) Following crude sampling by the initial bond in-plane rotation angle and out-of-plane excursion, a refined saddle point search is performed using a modified conjugate gradient method [14]. The modification formally defines quasienergy as a sum of squared values of the forces applied to all atoms. Then a standard minimization algorithm is applied to this quasienergy and searches for all points where the energy gradient is zero. Minima and maxima of the true energy are excluded afterwards, leaving the saddle points of interest. The gradients of the quasienergy are calculated analytically for the Tersoff-Brenner potential [15], to ensure a fast search, essential for the investigation of larger systems with a broader range of parameters.

E^* values are computed for 61 chiral angles $\chi \in [0; \pi/3]$, and strain of 51 magnitudes $\varepsilon \in [0; 0.05]$, for each of the 24 branches: 3 (bond choices) times 2 (left and right rotation directions) times 4 (modes S, S_{-+}, S_{++}, or S_+). The computed configurations are close to those described above, with the rotation angle near $\pi/4$. However, for a given strain ε, comparison and identification of the lowest-energy channel is simpler in the "extended zone scheme" (analogous to the conventional representation of the band structure in crystals), where $\chi \in [0; 2\pi]$ (Fig. 2). Physically, this corresponds to rotating only one trial bond in a single (right) direction, via all possible modes, with the tension direction varying around the full 2π circle. Obviously at $\varepsilon = 0$ there is no χ dependence. The results for $\varepsilon = 0.05$ are shown as a four-branch function with each branch corresponding to a particular mode.

The E^* dependence on the tension direction χ is evident and varies between the modes. For convenience, we choose the trial bond so that most interesting low-level transitions fall into $\chi \in [0; \pi/6]$, a standard chirality range. From a physical point of view, all modes, bond types, and rotation directions provide simultaneous, parallel channels for the relaxation in the lattice. The fastest of them dominates and determines the observable yield under tension, i.e., the lower envelope of the shown curves is

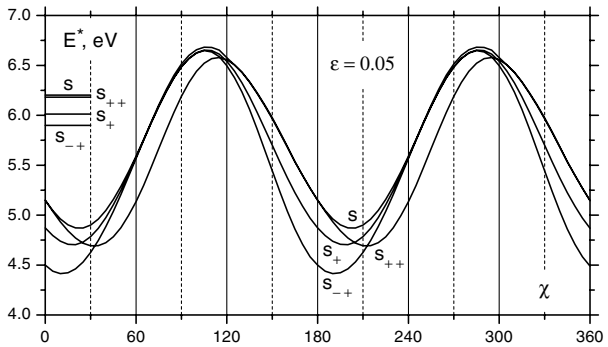

FIG. 2. Activation barrier E^* for the defect formation in a nanotube as a function of chirality χ, for a tensile strain $\varepsilon = 0.05$ (short horizontal segments correspond to $\varepsilon = 0$). Periodic dependence is evident in this "extended zone scheme." Different branches are marked according to the transition state modes.

mainly of interest. At this strain level, S_{-+} provides the lowest-energy path for the SW defect for all distinguishable chiralities $\chi \in [0; \pi/6]$. This is consistent with earlier observations (Fig. 1b in Ref. [8]) and additional molecular dynamics (MD) simulations: one atom often swinging inward and another outward. However, high temperature (near 2000 K) in MD makes it difficult to clearly identify the geometry and the actual height of the barrier. Here, the corresponding E^*_{-+} attains its minimum at the strain orientation $\chi = 11°$, indicating that the weakest tube must be closer to zigzag type ($\chi = 0$), very different from the thermodynamic assessment based on E_f that has a minimum at $\chi = 30°$ (armchair CNT). On the other hand, the highest barrier is observed at $\chi = 30°$, suggesting the lowest probability of failure for armchair tubes, again in contrast with the position $\chi = 0$ for maximum E_f. The reduction of energy by tensile strain can be understood in similar ways for the final (E_f) and transition (E^*) states. They both behave similar to dilatation centers in the lattice (an instantaneous, fluctuating one in the case of transition) with the largest energy reduction achieved by tension along the dilatation axis. The final SW bond is aligned at $30° + 90° = 120°$ from $\mathbf{a}_1$, and the tension in this direction occurs for $\chi = 30°$ (hence, minimum of E_f). In transition, the bond is oriented at $30° + 45° = 75°$ from $\mathbf{a}_1$, so the minimum for E^* could be expected for the tension applied at this angle, that is for $\chi = -15°$. At the actual E^*-minimum position $\chi = 11°$, the strain partially reduces the transition dilatation energy, and partially promotes its further rotation flip towards the final state. The difference of dilatation directions in the final SW and the transition is the likely cause of the shift in chiral behavior of E_f and E^*.

Computed E^* depend on strain ε almost linearly, for all the modes and chiral angles. Figure 3a depicts the branches of $E^*(\chi)$ computed at higher strain $\varepsilon = 0.1$, where the minimum remains at $\chi = 11°$, while near the maximum at $\chi = 30°$ mode S_{++} becomes competitive. The added plot of $E_f(\chi)$ illustrates again the qualitative difference between the kinetics of yield (E^*) and thermodynamic stability (E_f) in their dependencies on χ. The clear phase shift in correlation of the E^* with respect to E_f (Fig. 3a) demonstrates a peculiar example of the classic Evans-Polanyi rule [16]. In its original chemical context, it recognizes the linear relationship between activation energy and the heat of reaction. In our case, due to the symmetry difference between the transition and the final SW defect, there is a large χ-phase shift between the thermodynamic (E_f) and the actual rate determining (E^*) quantities.

The distinct periodicity of $E^*(\chi)$ and $E_f(\chi)$, and their approximately linear dependence on ε, call for analytical approximations (in eV):

$$E^*_{-+}(\varepsilon, \chi) = 5.9 - 7.4\varepsilon - 22\varepsilon \sin(2\chi + 68°) \quad (1a)$$

$$E^*_{++}(\varepsilon, \chi) = 6.2 - 11\varepsilon - 19\varepsilon \sin(2\chi + 25°) \quad (1b)$$

We omit equations for the modes S and S_+. We should mention that similarly large E^* have been discussed previously [10,13]. Moreover, the provided above values of $E^*_{-+}(\varepsilon, \chi = \pi/6)$ agree very well with this particular subset obtained differently in [8].

Now the physical consequences of these results can be discussed. First we note that the thermodynamic requirement for the defect formation ($E_f = 0$) is met sooner, at lower strain than is necessary for any detectable kinetic rate of yield. For example, the data at $\varepsilon = 0.1$ in Fig. 3a shows already negative E_f for most of the chiralities, but still prohibitively large E^*. Therefore, at strains large enough to sufficiently reduce the barrier, E_f is already negative, and defect formation is irreversible. The only criteria for failure (more accurately, first nucleation of failure, the primary SW defect) becomes kinetic: Within laboratory time Δt, at what strain ε does the probability P of the SW event in a given sample become significant? Quantitatively,

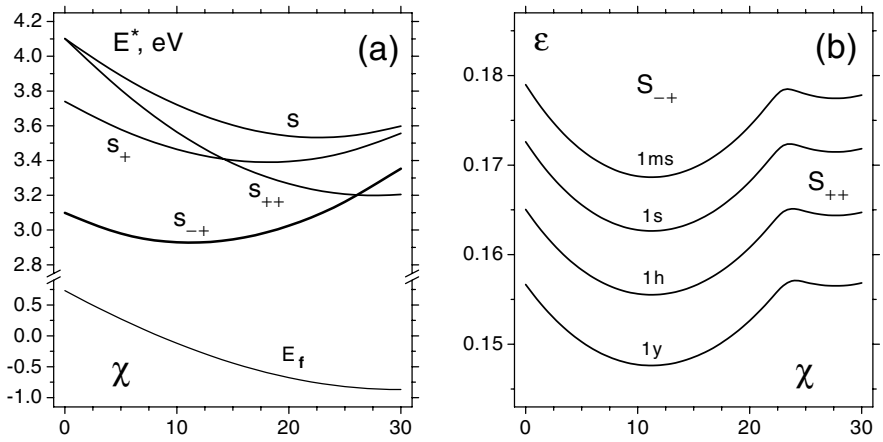

FIG. 3. In (a), the lowest activation energy (thick line) dependence on chirality is shifted with respect to the formation energy (E_f, bottom line), which at the strain $\varepsilon = 0.1$ is mostly negative. (b) Yield strain as a function of chirality, computed for different failure-expectation times, 1 ms, 1 s, 1 h, and 1 y as marked.

$$P = \nu \Delta t N_B/3 \sum_m \exp[-E_m^*(\varepsilon, \chi)/k_b T] \sim 1, \quad (2)$$

where index m numbers the modes. The coefficient $1/3$ here is due to the fact that only one-third of the bond orientations is normally prone to SW flip. Let us assume for a rough estimate, room temperature $T = 300$ K, the attempt frequency $\nu = k_b T/h = 10^{13}$ s^{-1} [16], a CNT length $L = 1$ μm, and diameter $d = 1.4$ nm. The total number of bonds is $N_B = 180Ld/\text{nm}^2$. Substituting these values together with the Eqs. (1) into Eq. (2), we compute the critical strain ε for the chosen times of yield, from $\Delta t = 1$ ms to $\Delta t = 1$ y, as shown in Fig. 3b. The effect of chirality on the yield strain is evident, while the specific choices of the test time, the sample size, and the frequency factor are mitigated by the logarithmic dependencies. Overall, Fig. 3 illustrates how our theory allows one to derive yield strength from interatomic forces (Tersoff-Brenner [15] in our case). More precise input from first principles calculations can refine the quantitative values for the specific material. However, the proposed approach will still be valid.

In summary, we have presented the first kinetic approach to CNT strength, predicting the yield strain range, the significant role of chiral symmetry, and the role of temperature. We believe that the presented theory can also serve as a framework for the treatment of failure nucleation in other crystals. With regard to quantitative predictions, we note that, for any particular CNT and conditions, further refinement of E^* values can be achieved by more accurate tight binding or *ab initio* treatment of chemical bonds. Since computing the overall landscape of $E^*(\varepsilon, \chi)$ for all various strains, chiralities, and modes remains impractical for *ab initio* methods, we employ a classical force field. This leads to yield strain near 17% corresponding to tensile strength of 150–180 GPa, assuming the CNT Young's modulus 1 TPa [4,17]. It compares well with reported experimental data of 4%, 5%, 16%, and 17% [18]. Here we deliberately discuss only ideal samples, pristine graphene, and CNT; factors such as preexisting defects, chemical environment, nonuniform load transfer, or *in situ* damage by an electron beam can reduce the measured yield level. These factors can be accounted for on a case by case basis, which obscures any general conclusions. The ideal defect-free sample, improbable in macroscopic scale, is more realistic as a nanoscale whisker or tubule.

This work was supported by the AFOSR and Materials Directorate, Air Force Research Laboratory, and by the Office of Naval Research.

*Corresponding author.
Email address: biy@rice.edu

[1] M. Marder and J. Fineberg, Phys. Today **49**, 24 (1996).
[2] V. Bulatov, F. F. Abraham, L. Kubin, B. Devincre, and S. Yip, Nature (London) **391**, 669 (1998).
[3] B. I. Yakobson, Phys. Rev. Lett. **67**, 1590 (1991).
[4] B. I. Yakobson and Ph. Avouris, in *Carbon Nanotubes,* edited by M. S. Dresselhaus, G. Dresselhaus, and Ph. Avouris (Springer-Verlag, Berlin, 2001), pp. 287–327; see also *Carbon Nanotubes,* edited by T. W. Ebbesen (CRC Press, Tokyo, 1997).
[5] R. H. Baughman, C. Cui, A. A. Zakhidov, A. G. Rinzler, and S. Roth, Science **284**, 1340 (1999); R. Gao, Z. L. Wang, Z. Bai, W. A. de Heer, L. Dai, and M. Gao, Phys. Rev. Lett. **85**, 622 (2000); B. Vigolo *et al.,* Science **290**, 1331 (2000).
[6] J. Tersoff and R. S. Ruoff, Phys. Rev. Lett. **73**, 676 (1994); B. I. Yakobson, C. J. Brabec, and J. Bernholc, Phys. Rev. Lett. **76**, 2511 (1996).
[7] B. I. Yakobson, Appl. Phys. Lett. **72**, 918 (1998).
[8] M. Buongiorno Nardelli, B. I. Yakobson, and J. Bernholc, Phys. Rev. B **57**, R4277 (1998).
[9] M. B. Nardelli, B. I. Yakobson, and J. Bernholc, Phys. Rev. Lett. **81**, 4656 (1998).
[10] P. Zhang, P. E. Lammert, and V. H. Crespi, Phys. Rev. Lett. **81**, 5346 (1998); H. F. Bettinger, T. Dumitrica, G. E. Scuseria, and B. I. Yakobson, Phys. Rev. B **65**, 041406 (2002).
[11] B. I. Yakobson, Ge. G. Samsonidze, and G. G. Samsonidze, Carbon **38**, 1675 (2000); Ge. G. Samsonidze, G. G. Samsonidze, and B. I. Yakobson, Comput. Mater. Sci. (to be published).
[12] B. C. Pan, W. S. Yang, and J. Yang, Phys. Rev. B **62**, 12 652 (2000).
[13] Similar modes have been detected in quantum *ab initio* studies of fullerenes: S_+ and S_{++}, respectively, in R. L. Murry, D. L. Strout, G. K. Odom, and G. E. Scuseria, Nature (London) **366**, 665 (1993); B. R. Eggen, M. I. Heggie, G. Jungnickel, C. D. Latham, R. Jones, and P. R. Briddon, Science **272**, 87 (1996). *Ab initio* results from work in progress are close to 6.2 eV in Eggen *et al.,* with no mechanical load, and decrease accordingly under tension [H. F. Bettinger, K. N. Kudin, G. E. Scuseria, and B. I. Yakobson (unpublished)]. In highly curved fullerenes, the atom is more likely to be shifted outwards from the cage, and the convex S_{++} and S_+ can be more favorable than the flat, in-plane S or S_{-+}. The coordinate constraints, equivalent to the addition of virtual forces in the system, could distort the resulting S_{++}. Our constraint-free method locates the unperturbed transition states.
[14] G. G. Samsonidze and Ge. G. Samsonidze (unpublished).
[15] J. Tersoff, Phys. Rev. B **37**, 6991 (1988); D. W. Brenner, Phys. Rev. B **42**, 9458 (1990).
[16] S. Glasstone, K. J. Laidler, and H. Eyring, *The Theory of Rate Processes* (McGraw-Hill, New York, 1941).
[17] K. N. Kudin, G. E. Scuseria, and B. I. Yakobson, Phys. Rev. B **64**, 235406 (2001).
[18] M. R. Falvo, G. J. Clary, R. M. Taylor, V. Chi, F. P. Brooks, S. Washburn, and R. Superfine, Nature (London) **389**, 582 (1997); H. D. Wagner, O. Lourie, Y. Feldman, and R. Tenne, Appl. Phys. Lett. **72**, 188 (1998); M. F. Yu, B. S. Files, S. Arepalli, and R. S. Ruoff, Phys. Rev. Lett. **84**, 5552 (2000); B. G. Demczyk, Y. M. Wang, W. Han, M. Hetman, A. Zettl, and R. O. Ritchie, Bull Am. Phys. Soc. **46**, 11 774 (2001).